Molecular Crystals and Liquid Crystals
Publication details, including instructions for authors and subscription information:
http://www.tandfonline.com/loi/gmcl20

Optical Vortex Generation in Nematic Liquid Crystal Light Valves

R. Barboza [a b], U. Bortolozzo [a], G. Assanto [b] & S. Residori [a]
[a] INLN, Université de Nice-Sophia Antipolis, CNRS, Valbonne, France
[b] NooEL (Nonlinear Optics and OptoElectronics Laboratory), University Roma Tre, Rome, Italy
Published online: 02 Apr 2013.

To cite this article: R. Barboza, U. Bortolozzo, G. Assanto & S. Residori (2013) Optical Vortex Generation in Nematic Liquid Crystal Light Valves, Molecular Crystals and Liquid Crystals, 572:1, 24-30, DOI: 10.1080/15421406.2012.763206

To link to this article: http://dx.doi.org/10.1080/15421406.2012.763206

Mol. Cryst. Liq. Cryst., Vol. 572: pp. 24–30, 2013

ISSN: 1542-1406 print/1563-5287 online
DOI: 10.1080/15421406.2012.763206

Taylor & Francis
Taylor & Francis Group

Optical Vortex Generation in Nematic Liquid Crystal Light Valves

R. BARBOZA,[1,2,*] U. BORTOLOZZO,[1] G. ASSANTO,[2] AND S. RESIDORI[1]

[1]INLN, Université de Nice-Sophia Antipolis, CNRS, Valbonne, France
[2]NooEL (Nonlinear Optics and OptoElectronics Laboratory), University Roma Tre, Rome, Italy

A nematic liquid crystal light valve (LCLV) is made by using a photosensitive material as one of the cell-confining walls. The liquid crystals (LCs) are homeotropically aligned and with a negative anisotropy; therefore, they naturally produce topological defects when they reorient under the application of an electric field. In our work, we show that by sending circularly polarized light beams onto the photosensitive wall of the light valve, it is possible to locally induce the reorientation and to generate vortex-like defects that remain, each stable and trapped at the chosen location. We demonstrate the ability of the system to create optical vortices with opposite topological charge that, consistently with angular momentum conservation, both derive from the same defect created in the LC texture.The efficiency of the spin-to-orbital angular momentum conversion is measured as a function of the system control parameters, namely the low-frequency electric field applied to the light valve and the intensity of the optical beam inducing the matter defect.

Keywords Liquid crystal light valves; optical vortices; spin-to-orbital angular momentum conversion; topological defects

1. Introduction

Optical vortices, or wavefront dislocations, have been identified as the singular points where a complex field goes to zero and around which the phase screws up as an n armed spiral, with n being the topological charge [1,2,3]. Recently, the presence of a single optical vortex, appearing as a phase singularity in low-order Gauss–Laguerre beams, has been highlighted in view of useful applications, as the exchange of angular momentum between light and matter [4], the realization of optical tweezers [5,6,7], quantum computation [8], and improvement in astronomical imaging [9]. Up to now, the controlled generation of optical vortex beams has been mainly realized by using spiral-phase plate, SSPs, [10] or diffractive optical elements, DOEs, [11,12]. Among these schemes, one can note that some devices, for instance, SSPs, lack in tunability, while others, such as DOEs, can exhibit efficiency problems. Another approach has been, recently, proposed that relies on preimposed radial director orientation in liquid crystal (LC) samples, so-called, q-plates [13]. This method

*Address correspondence to R. Barboza, NooEL (Nonlinear Optics and OptoElectronics Laboratory), University Roma Tre, Via della Vasca Navale 84, Rome, Italy. Tel: +39 06 5733 7045; Fax: +39 06 5733 7101. E-mail: raouf.barboza@uniroma3.it

provides both tunability and high efficiency. However, one of the problems encountered in using these devices is that the LC alignment can cause some beam deformation and a consequent loss in the quality of the generated optical vortices [14].

In our work, we propose a different method that tackles all these problems by using liquid crystal light valves (LCLVs) with homeotropic anchoring conditions and a photosensitive wall [15]. The incoming light beam creates a defect within the cell, which, in turn, couples the orbital and the spin component of the angular momentum. Thanks to the transverse component of the generated electric field across the LC layer, an effective potential is induced that is able to pin the defect at the chosen location. Therefore, the LCLV method enables the controlled and reliable induction of reconfigurable defects in the LC texture, which, in turn, comports the controlled generation of optical vortex beams.

2. Description of the Device

The LCLV is schematically represented in Fig. 1. It is composed of an LC layer in between two slabs of 25 $\times$ 25-mm^2 transverse size. The input face is made of a transparent photoconductor bismuth silicon oxide $Bi_{12}SiO_{20}$ (BSO) with 1-mm thickness, whereas the other face is made of a glass plate of the same width and 0.7-mm thickness. The interior surface of the glass plate and the external surface of the BSO are coated with indium tin oxide, ITO, a commonly used transparent conductor. The noncoated face of the BSO and the coated face of the glass plate are treated in order to provide provide homeotropic anchoring conditions. The LCLV is, then, assembled with 15-μm spacers and filled with a nematic LC with negative dielectric anisotropy (MLC6608).

The photoconductive BSO layer acts as an optical tunable impedance realizing a voltage divider arrangement that enable us to spatially tune the effective voltage across the LC layer by using a proper illumination profile. As an example, in Fig. 1, the local distribution of the director under local illumination with a Gaussian beam is depicted. The phase and intensity profiles at the input and output of the LCLV are represented in the left and right part of the figure, respectively.

3. Topological Defects in Homeotropically Aligned Cells

When a nematic LC cell is biased and the voltage across the nematic layer is above the Fredericks transition voltage V_{FT}, the molecules reorient. This is because the torque

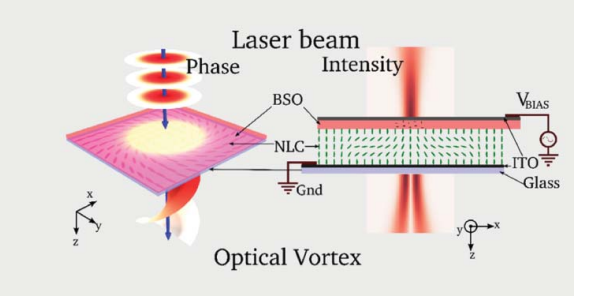

Figure 1. Schematic sketch of the liquid crystal light valve and of the process of vortex induction. In the left part of the figure are shown the phase profiles of the input and output beam. On the right are represented their respective intensity profiles. The corresponding alignment of the nematic director is depicted from a top view (left) and a from a y-cut in the middle of the valve (right).

stemming from the elastic forces linking together the LC molecules is overcome by the electric torque due to the applied voltage. If the nematic LC layer is homeotropically aligned and the dielectric anisotropy is negative, then the molecules will rotate perpendicularly to the applied electric field. Due to the 2π degeneracy of the direction of the reorientation, the molecules (actually the projection of the director on the x–y plane) will align in random directions, causing the formation of defects in the texture of the nematic layer. These defects are in general umbilics (nonsingular) with a Frank index ± 1 [16]. Correspondingly, the winding number, that is, the degree of the singularity enclosed in a loop around the defect in the transverse x–y plane is ± 1. Both the position and the number of defects created by the Fredericks transition are uncontrollable, since the system is driven from the unstable condition through random fluctuations of the director around the homeotropic state. Umbilics with the same winding number will repeal each other and those with opposite winding number will attract and annihilate. Through this coarsening process [2], the gas of vortices relaxes towards an equilibrium state, exhibiting a uniform texture or a pair of defects (eventually, one defect of the pair can be hidden by boundary effects) [17]. The remaining umbilic can, then, be used to generate optical vortices [18,19]; however, the spontaneous relaxation dynamics of the vortex gas does not allow any external control of the system.

To overcome these difficulties and limitations, it is necessary to provide a reliable way to generate the umbilic, which should be addressable by a specific control method and hence generated when needed and where it is needed on the LC cell. For this purpose, we rely on the LCLV, whose behavior is detailed in the paragraph above. The cell is biased, initially, in order to have the effective voltage across the LC layer slightly below the Fredericks transition voltage, with the intent to avoid the spontaneous formation of umbilics. When a light beam of Gaussian shape is shone onto the photoconductive side of the LCLV, due to the photo-generated charges, the impedance of the BSO decreases, making it more conductive where the intensity is larger. The effective voltage across the LC layer acquires, therefore, a bell-shaped profile, higher in the center. By increasing the bias voltage or the beam intensity, the peak value of the effective voltage can, eventually, go beyond the Fredericks voltage. As a consequence, the molecules will tilt first toward the x–y plane, but not randomly as in an uniformly biased cell (normal homeotropic one). The radial symmetry of the voltage drop will give rise to a transverse component of the electric field, also with the same radial profile. This biases the system, making the nematic director to follow the same symmetry while reorienting, and giving birth to a single singularity in the texture of the nematic layer.

A single umbilic defect obtained with this method is shown in Fig. 2. The profile of the director in the x–y plane is schematically sketched in Fig. 2(a), whereas in Fig. 2(b), the umbilic is observed with an analyzer under circular polarized white light. A spatially resolved polarimetry [20] of the defect is obtained by using quarter wave plates to analyze

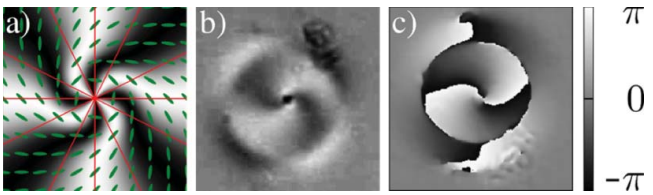

Figure 2. (a) Schematic representation of the nematic alignment in the x–y plane.The (red) solid lines represent the direction of the generated transverse component of the electric field. (b) Umbilic-like defect observed with an analyzer under circular polarized white light. (c) Spatially resolved polarimetry of the defect showing its phase profile.

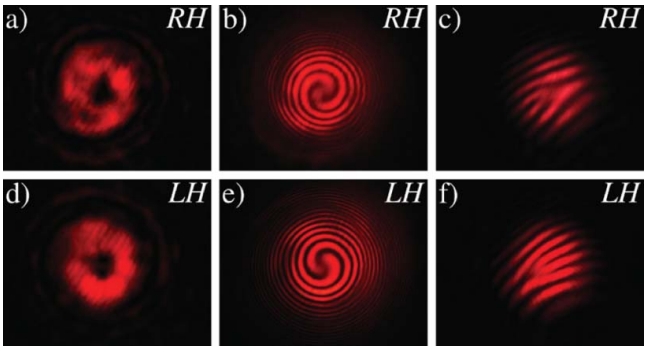

Figure 3. Profiles of the generated optical vortices: (a–d) typical doughnut profile of order 2 for the LH/RH-polarized Laguerre–Gauss beam LG_0^2 obtained with an RH/LH input beam. Corresponding (b–e) spherical and (c–f) plane-wave interference patterns of the −2/+2-charged optical vortices.

the local birefringence properties of the distorted layer. The result is shown in Fig. 2, where the polarimetric profile shows that the created defect has an umbilic-like structure and a winding number $q = +1$, thus mimicking the transverse electric field distribution.

4. Umbilic and Light Interaction: Spin-to-Orbital Angular Momentum Conversion

Due to the azimuthal profile of the molecular reorientation, the optically induced defect acts like a q-plate. This is a specifically designed LC cell where a radial or twisted alignment of the molecules is obtained by rubbing circularly the glass plates forming the cell [13]. The q-plate is able to perform spin-to-orbital angular momentum conversion for an incoming input beam [21]. In fact, if we neglect diffraction inside the thin LC layer, and consider only the transverse component of the electric field, we can write the Jones matrix of this optical element as

$$M = \begin{bmatrix} 1 & 0 \\ 0 & 1 \end{bmatrix} \cos\frac{\delta}{2} + i \begin{bmatrix} \cos 2\theta & \sin 2\theta \\ \sin 2\theta & -\cos 2\theta \end{bmatrix} \sin\frac{\delta}{2}, \tag{1}$$

with δ being the overall effective phase shift between the (local) ordinary and (local) extraordinary component of the electric field, given by $\delta = 2\pi \frac{d}{\lambda}(\bar{n} - n_o)$, where d is the thickness of the LC layer,

$$\bar{n} = \frac{1}{d} \int_0^d n(\psi) dz, \tag{2}$$

and

$$n(\psi) = \frac{n_e n_o}{\sqrt{n_o^2 \sin^2 \psi + n_e^2 \cos^2 \psi}} \tag{3}$$

is the local refractive index seen by the extraordinary component of the electric field. Here, ψ is the LC tilt angle, n_o and n_e are the ordinary and extraordinary refractive index of the LC, respectively, and ψ and θ are the polar and azimuthal coordinate of the nematic director, respectively.

We will assume for simplicity $\theta = q\xi + \theta_o(r, z)$, where ξ is the local coordinate, and $\psi = \psi(r, z)$. For a circularly polarized input $\vec{e}_\sigma = A\frac{1}{\sqrt{2}}(\vec{x} + i\sigma\vec{y})$, where $\sigma = +1$ stands

for left-handed (LH) and $\sigma = -1$ for the right-handed (RH) circular polarization, and dropping down irrelevant phase factors, it can be shown that the output beam is given by

$$\vec{E} = A\cos\frac{\delta}{2}\vec{e}_{\sigma} + \exp(2iq\sigma\xi)A\exp(2i\sigma\theta_{\mathrm{o}})\sin\frac{\delta}{2}\vec{e}_{-\sigma}. \tag{4}$$

As it appears clearly from Equation (4), the incoming circularly polarized field is converted to a beam with opposite polarization and with an additional helical phase factor $\exp 2iq\xi$ through a conversion factor $\sin^2(\delta/2)$. As a matter of fact, an incoming LH/RH circularly polarized Gaussian input beam entering the LCLV will exit, for the ideal case $\delta = \pi$, with the RH/LH circular polarization and with an additional helical phase with winding number ± 2 (in our case q = 1). The acquired helical phase profile changes the structure of the amplitude of the output field. Indeed, the amplitude has to go to zero at the center of the beam in order to have a single-valued field. This gives birth to beams called optical vortices, that is, beams characterized by a phase singularity on their axis of propagation.

A rapid check on the amount of the momentum transferred to the defect shows us that we are in the presence of conversion of spin angular momentum (from the input beam) to orbital angular momentum (to the output beam). Indeed, the angular momentum per photon for the input beam is $\sigma\hbar$, whereas for the output beam, we have to count $\sigma\hbar\cos^2(\delta/2)$ for the σ polarized component (the spin part) and $-\sigma\hbar\sin^2(\delta/2) + 2\sigma\hbar\sin^2(\delta/2)$ for the $-\sigma$ polarized component (spin and orbital part). It appears clearly that the net change in the angular momentum is zero; hence, we are in the case of spin-to-orbital angular momentum conversion. Since the total torque density on the defect is proportional to the net change in the optical angular momentum [21], the incident beam does not exert any torque on the umbilical defect. The only mechanism pinning the defect at its place is the transverse electric field stemming from bell-shaped profile of the effective voltage across the LCLV. Indeed, this creates an effective potential able to stabilize the defect [15]. This mechanisms underlines the key role of the LCLV in providing an effective method to generate stable and controlled optical vortices.

5. Experimental Results

In the experiment, the LCLV is filled with the nematic LC MLC6608 (Merck), which exhibits a negative dielectric anisotropy $\Delta\varepsilon = -4.2$ and a Fredericks transition voltage $V_{\mathrm{FT}} = 3.2$ V. The LCLV is biased with a low-frequency (sine wave) voltage in order to avoid ion formation, which can have a detrimental effect on the LC and the whole cell. The frequency is tuned to 100 Hz in order to obtain an optimal response of the LCLV to the incoming light. The ordinary and the extraordinary refractive index are, respectively, $n_{\mathrm{o}} = 1.4637$ and $n_{\mathrm{e}} = 1.5338$, giving a maximum reachable phase shift of about 3.3π at 633 nm (we use a HeNe laser source) and for a thickness $d = 15$ μm of the LC layer. The π phase shift is reached at $\psi \approx 34^{\circ}$.

A circularly polarized Gaussian beam, either right-handed, RH, or left-handed, LH, with a waist of 25 μm is sent onto the LCLV. The setup is arranged in order to have a Mach–Zehnder interferometer with the LCLV on one arm. A quarter wave plate and a polarizer are placed after the LCLV in order to filter out the incoming circular beam, so that at 0 V, the measured output intensity is zero. For a 0.55 mW input power and a driving voltage of 24 V, the output beam intensity profile and two types of interference patterns, with a spherical- and a plane-wave reference beam, are recorded. The results are displayed in Fig. 3 for the RH input (Figs 3(a)–(c)) and the LH input (Figs 3(c)–(e)). In both cases, the

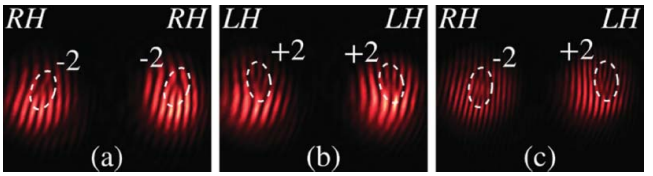

Figure 4. Interferogram of two independent optical vortices: (a) RH-RH, (b) LH-LH, and (c) RH-LH polarized input beams. The encircled areas show the dislocations in the fringe patterns. The changes of the dislocation direction depend on the sign of the topological charge of the induced vortices.

output beam exhibits a doughnut profile of the intensity, Figs 3(a)–(d). The two spiral arms for the spherical wavefront interference patterns, Figs 3(b)–(e), or the two dislocations in the plane wavefront interference fringes, Figs 3(c)–(f), confirm the fact that the output beam has, in both cases, a phase singularity with winding number 2 in modulus. The direction of the rotation of the spirals arms (Figs 3(b)–(e)) or the orientation of the dislocation lines (Figs 3(c)–(f)) are reversed for the two types of polarization, thus confirming that for the LH/RH input, the output is RH/LH-polarized with topological charge $+2/-2$.

To test the versatility of the system and its capabilities in terms of density of controlled defects, we have sent onto the LCLV two Gaussian beams with the same waist as before and with their mutual distance of about the same length as their waist. The plane-wave interference patterns are recorded for different combinations of the input polarizations: RH-RH, LH-LH, anf RH-LH. Figure 4 displays the robust generation of adjacent optical vortices, irrespective of their topological charge. This possibility enables the future generation of dense arrays of independent singular optical beams.

Finally, in Fig. 5, we display the efficiency of the conversion process. For this purpose, we have recorded the intensity of the output converted beam for different levels of the input power, ranging from 0.25 mW to 5 mW and by sweeping the driving voltage from 0 V up to 100 V (peak value). First, we fix the input beam intensity and then the voltage is increased slowly to the desired value in order to prevent the formation of other defects. In the meantime, the output power is recorded with a photodiode. For small input power, around 0.25 mW, the vortex appears at about 18 V, that is, the threshold of the LCLV is greater than V_{FT} due to the voltage drop over the BSO layer. For the highest power, the vortex appear sooner due to the fact that the incoming beam increases the background conductivity of the BSO, lowering the effective threshold of the cell. For each response curve, the first peak is reached when the overall phase shift is an odd multiple of π, the maximum phase shift being 3.3π. A saturation effect is observed at high voltage.

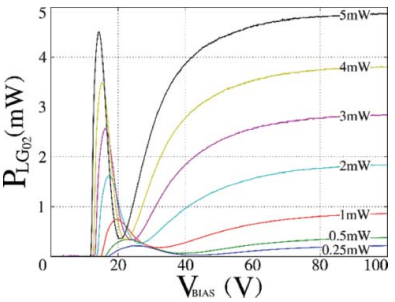

Figure 5. Dependency of the generated singular beam on the voltage applied to the LCLV. Labels on the curves refer to the power of the input Gaussian beam.

6. Conclusions

In conclusion, we have shown that a reliable and controllable method to generate optical vortex beams can be efficiently implemented by using a homeotropic LCLV. Thanks to the photoconductive wall of the light valve, the local illumination with a Gaussian light beam induces a bell-shaped profile of the effective electric field across the LC layer, which creates a topological defect and induces, at the same time, an effective potential able to pin the defect at its place. The created defect acts as an optical element able to convert spin-to-orbital angular momentum. Therefore, if the input beam is circularly polarized, the outgoing beam acquires a phase singularity and transforms into an optical vortex beam. The large transverse size of the LCLV and its capability to host a large number of topological defects, together with the ability to control the defect position, open the way to the exploitation of the system for the generation of large arrays of singular beams.

Acknowledgments

UB and SR acknowledge financial support from the ANR international program, project ANR-2010-INTB-402-02 (ANR-CONICYT39), "COLORS." GA acknowledges travel funding from the Program for Internationalization at University Roma Tre.

References

[1] Nye, J. F., & Berry, M. V. (1974). *Proc. R. Soc. Lond. A*, *336*, 165.
[2] Pismen, L. M. (1999). *Vortices in Nonlinear Fields*, Oxford Science Publications: New York.
[3] Soskin, M. S., & Vasnetov, M. V. (2001). Singular optics, In: E. Wolf (Ed.), Progress in Optics, Vol. 42, Elsevier: New York, pp. 219–276.
[4] Allen, L., Allen, L., Beijersbergen, M. W., Spreeuw, R. J. C., & Woerdman, J. P. (1992). *Phys. Rev. A*, *45*, 11.
[5] Simpson, N. B., Allen, L., & Padgett, M. J. (1996). *J. Mod. Opt.*, *43*, 2485.
[6] Curtis, J. E., Koss, B. A., & Grier, D. G. (2002). *Opt. Commun.*, *207*, 169.
[7] Grier, D. G. (2003). *Nature*, *424*, 810.
[8] Arnaut, H. H., & Barbosa, G. A. (2000). *Phys. Rev. Lett.*, *85*, 286.
[9] Tamburini, F., Anzolin, G., Umbriaco, G., Bianchini, A., & Barbieri, C. (2006). *Phys. Rev. Lett.*, *97*, 163903.
[10] Beijersbergen, M. W., Coerwinkel, R. P. C., Kristensen, M., & Woerdman, J. P. (1994). *Opt. Commun.*, *112*, 321.
[11] Bazhenov, V. Y., Vasnetsov, M. V., & Soskin, M. S. (1990). *JETP Lett.*, *52*, 429.
[12] Sacks, Z., Rozas, D., & Swartzlander, G. A. (1998). *J. Opt. Soc. Am. B*, *15*, 2226.
[13] Marrucci, L., Manzo, C., & Paparo, D. (2006). *Phys. Rev. Lett.*, *96*, 163905.
[14] Bekshaev, A. Ya., & Sviridova, S. V. (2010). *Opt. Comm.*, *283*, 4866.
[15] Barboza, R., Bortolozzo, U., Assanto, G., Vidal-Henriquez, E., Clerc, M. G., & Residori, S. (2012). *Phys. Rev. Lett.*, *109*, 143901.
[16] Chandrasekhar, S. (1977). *Liquid Crystals*, Cambridge University Press: New York.
[17] Dierking, I., Marshall, O., Wright, J., & Bulleid, N. (2005). *Phys. Rev.*, *E 71*, 061709.
[18] Brasselet, E., & Loussert, C. (2011). *Opt. Lett.*, *36*, 719.
[19] Brasselet, E. (2012). *Phys. Rev. Lett.*, *108*, 087801.
[20] Soskin, M. S., Denisenko, V. G., & Egorov, R. I. (2004). *Proc. SPIE*, 5458.
[21] Marrucci, L. (2008). *Mol. Cryst. Liq. Cryst.*, *488*, 148.